Alloys developed for high temperature applications

Eddy Agus Basuki, Djoko Hadi Prajitno, and Fadhli Muhammad

Articles you may be interested in

Improving hot corrosion resistance of two phases intermetallic alloy α_2-Ti$_3$Al/γ-TiAl with enamel coating
AIP Conference Proceedings **1805**, 070003 (2017); 10.1063/1.4974444

Co-based alloys design based on first-principles calculations: Influence of transition metal and rare-earth alloying element on stacking fault energy
AIP Conference Proceedings **1805**, 060004 (2017); 10.1063/1.4974440

Preface: Proceedings of the 1st International Process Metallurgy Conference, IPMC 2016
AIP Conference Proceedings **1805**, 010001 (2017); 10.1063/1.4974406

Industrial use of thermodynamic simulations in pyrometallurgy
AIP Conference Proceedings **1805**, 020001 (2017); 10.1063/1.4974407

Smelting furnace melt zone wall modification to cope higher production rate operation
AIP Conference Proceedings **1805**, 020005 (2017); 10.1063/1.4974411

Atmospheric leaching of nickel and cobalt from nickel saprolite ores using the Starved Acid Leaching Technology
AIP Conference Proceedings **1805**, 020002 (2017); 10.1063/1.4974408

Alloys Developed for High Temperature Applications

Eddy Agus Basuki[1,*], Djoko Hadi Prajitno[2] and Fadhli Muhammad[1]

[1] Department of Metallurgical Engineering, Faculty of Mining and Petroleum Engineering,
Institut Teknologi Bandung, Jl. Ganesha 10, Bandung 40132, Indonesia
[2] Nuclear Technology Center for Materials and Radiometry, National Atomic Agency of Indonesia

[*]Corresponding author: basuki@mining.itb.ac.id

Abstract. Alloys used for high temperatures applications require combinations of mechanical strength, microstructural stability and corrosion/oxidation resistance. Nickel base superalloys have been traditionally the prime materials utilized for hot section components of aircraft turbine engines. Nevertheless, due to their limited melting temperatures, alloys based on intermetallic compounds, such as TiAl base alloys, have emerged as high temperature materials and intensively developed with the main aim to replace nickel based superalloys. For applications in steam power plants operated at lower temperatures, ferritic high temperature alloys still attract high attention, and therefore, development of these alloys is in progress. This paper highlights the important metallurgical parameters of high temperature alloys and describes few efforts in the development of Fe-Ni-Al based alloys containing B2-(Fe,Ni)Al precipitates, oxide dispersion strengthening (ODS) ferritic steels and titanium aluminide based alloys include important protection system of aluminide coatings.

Keywords: superalloys, (Ni,Fe)Al precipitate, ODS ferritic steels, TiAl base alloys

INTRODUCTION

High temperature operations, such as those found in aircraft and land based turbine engines as well as boilers, require materials which have a good combination of mechanical properties, microstructural stability and corrosion resistance at relatively high temperatures. Especially for air craft turbine blades, these components are subjected to a number of extreme external conditions, such as high tensile loads and corrosive environments, all of which occur under thermal cycling conditions due to the relatively short cooling-heating cycle of the engines. Similarly, components in coal-fired power plants, such as heat exchangers, are exposed at high temperatures in environments containing corrosive species and particulates. Especially for fossil fuel engines operating at higher efficiency is demanded due to the depletion of global fossil fuel resources as well as requirement for reducing global warming. Thermodynamic principle has clearly suggested the requirement of higher operating temperatures for higher efficiency of the engines. Obviously, this will give further challenge to continuously improve high temperature alloys before brittle non-metallic materials, such as oxide systems, can be toughened.

The target for higher efficiency in coal-fired advanced ultra-super critical (A-USC) steam cycle needs advanced materials that capable to be operated at high temperatures (≥ 700°C) and pressures (≥ 350 bar) [1]. Advanced steels, stainless steels as well as nickel based alloys are considered as the materials that can fulfill this requirement. Turbine blades of aircraft engines are the parts that experience extreme operating conditions, both at high pressure (>40 bar) and temperatures (>1600°C) [2]. Materials used for these applications have been studied and developed rigorously, and the results may be shared for the application of high temperature alloys for land base turbine engines as well as steam power plant [3].

STRENGTHENING MECHANISMS OF HIGH TEMPERATURE ALLOYS

The strength of most alloys are normally decreases with temperatures, except some intermetallic compounds, such as γ'-Ni$_3$Al which increases with temperatures up to about 900°C [4]. At any temperature, pure metals are usually weak and easily attacked by corrosive environment. Therefore, metals are alloyed with other elements in order to have strengthening as well as corrosion resistance. For corrosion protection, the alloying elements, such as Cr, Al or Si, should be dissolved homogenously in the matrix of base metals, either Fe, Ni, Co or Fe-Ni so they have readiness to form protective scales of Al$_2$O$_3$, Cr$_2$O$_3$, SiO$_2$ on the surface of the alloys. In addition, the dissolved elements can provide strengthening to the alloys through solid solution strengthening. When addition of the alloying elements higher than their solid solubility limit, second or third phase precipitates can occur and these provide another mode of strengthening mechanism, *i.e.,* precipitation strengthening or hardening.

Precipitates of γ'-Ni$_3$(Al,Ti) has been well recognized as the main strengthener for nickel-based superalloys. The addition of carbon in Fe, Ni and Co based-alloys provide various types of carbides precipitates, such as M$_{23}$C$_6$, MC, M$_6$C, M$_7$C$_3$, where M occupied by refractory elements (Mo, W, V, Nb) or Cr, and these contribute to the additional precipitation strengthening for the alloys. When these carbides precipitate along grain boundaries, they increase the creep resistance of polycrystalline alloys. However, because the precipitates are metastable, they will coarsen when heated at high temperatures, so that the strength and creep resistance of the alloy decreases with time. Efforts have been done to involve more stable nano size oxide particles such as Y$_2$O$_3$, ThO$_2$ and ZrO$_2$ that can disperse homogenously in the alloy grains through mechanical alloying process [5]. This oxide dispersion strengthening (ODS) alloys have higher stability since the oxide particles will not coarsen. Other strengthening mechanisms that apply for room temperature applications, such as strain hardening and martensitic strengthening are not effective for high temperature applications due to recrystallization and grain growth phenomena.

ALLOY DEGRADATION AT HIGH TEMPERATURES

Movement of atoms or ions in the materials increases at high temperatures due to the involvement of activation energy. In addition, the concentration of vacancy that responsible for diffusion of atoms and ions increase exponentially with temperatures. Therefore, any changing that occur in alloys, both in the interior as well as on the surface of the materials that reduce their properties, increases significantly with temperatures. High temperature alloys are normally designed to reduce this changing. Oxidation, hot corrosion, creep, thermal fatigue and microstructural changing are modes of alloy degradation occur at high temperatures. Oxidation and hot corrosion are considered as the worst alloy degradation modes because of their close relation with environment that relatively difficult to control.

Combination of high temperature operation and contaminants in environment, such as sulfur, sodium, halides and vanadium, resulted in the formation of a dangerous high temperature corrosion mode named hot corrosion. Unlike high temperature oxidation that produce relatively uniform and highly predictable scales as corrosion products, this type of corrosion has pitting type with rapid rate and often unpredictable. Therefore, catastrophic failure of the components may occur due to this hot corrosion since the load-carrying ability of the material is reduced rapidly. Extensive studies have been conducted to investigate the phenomena of hot corrosion, especially in air-craft turbine engines [6,7,8].

Hot corrosion may be defined as accelerated attack of molten sodium salts and oxides mixture such as NaCl, Na$_2$SO$_4$ and V$_2$O$_5$ deposited from environment contaminants at high temperatures. Two forms of hot corrosion attack have been identified [9], *i.e.,* Type 1 hot corrosion, which is hot corrosion occur at high temperatures (850-950°C) or usually named as high temperature hot corrosion (HTHC), and Type 2 hot corrosion, which is hot corrosion that occur at relatively low temperatures (650-850°C) or normally called as low temperature hot corrosion (LTHC). Chemical composition of the alloys or coatings and environment contaminants as well as the operating temperatures will define the hot corrosion type that applies. In HTHC the dominant deposit is fused alkali salt, especially Na$_2$SO$_4$. This deposit formed as the results of reactions between SO$_2$ from the fuel combustion, NaCl from fuel or environment that close to coastal and H$_2$O as shown in Eq. (1) [6]:

$$2NaCl + SO_2 + H_2O + 1/2O_2 \rightarrow Na_2SO_4 + 2HCl \qquad (1)$$

At 850-950°C, the deposit will be in liquid phase so that it can cover the whole surface of the scales of the components. Na$_2$SO$_4$ that melts at about 880°C firstly react with the oxides in the protective scale, such as Cr$_2$O$_3$ or salt fluxing [9] and this leads to further oxidation of Cr that occasionally makes depletion of Cr in substrate underneath

the scale. Finally, oxidation will occur with the base metals, Fe or Ni, and produce porous scales. This oxidation will release elemental sulfur, and sulfides of base metals with low melting point will form. This causes peeling of the surface metals and the corrosion product is characterized by base metal oxide precipitates dispersed in a film of salt mixtures. Other fuel or atmosphere contaminants, such as vanadium and phosphorous, might mix together with Na_2SO_4 to produce lower melting point salt mixtures, so that increasing the degree of attack. Excess of NaCl can produce eutectic of NaCl and Na_2SO_4 that melt at 620°C. The LTHC occur at lower temperatures and characterized by pitting type attack. This corrosion is mainly due to the formation of low melting point eutectics of the mixture between Na_2SO_4 and base metal sulfates, such as $NiSO_4$ and $FeSO_4$. The eutectics have melting points of about 550°C. $NiSO_4$ and $FeSO_4$ formed as the result of the reaction between base metal oxides and SO_3 in the combustion gas. High partial pressure of SO_3 is required for the LTHC to proceed.

PROTECTION OF THE ALLOYS

In order for scales can act as protective layer on alloy surface, they should consist of oxides that thermodynamically stable at high temperature, have high melting point, low vapor pressure, slow formation rate, high adherence on the alloy surface, low thermal expansion, and good erosion resistance. At temperatures higher than 560°C, Fe in iron based alloys oxidized to form FeO. However, this oxide has high oxidation rate, therefore FeO is a non-protective scale, and similarly NiO in Ni-based alloys and TiO_2 in titanium based alloys. Almost all high temperature alloys utilized protective scales of Al_2O_3, Cr_2O_3 or SiO_2. Among these three protective scales, Al_2O_3 has higher stability at temperatures higher than 1000°C, since Cr_2O_3 or SiO_2 can form high volatile oxides, such as CrO_3, However, Cr_2O_3 has better protective scale for hot corrosion mode.

The primary reason for the addition of aluminium in Fe and Ni based alloys is to provide alloy strength through formation of coherent intermetallic phase precipitates of γ'-Ni_3(Al). Moreover, the maximum chemical content of aluminium necessary to optimize the strength in these alloys is considered too low to produce the protective scale of Al_2O_3 [10]. Furthermore, it has been reported [11] that increasing the aluminium content in nickel-based superalloys reduces the solubility of chromium in the matrix and therefore decreases the hot corrosion resistance of the material. Therefore, to provide superalloys with high strength and good oxidation and corrosion resistance, coatings based on the nickel aluminide β-NiAl are applied on the surface of the materials [6].

Fe AND Ni BASED ALLOYS FOR HIGH TEMPERATURE APPLICATIONS

Iron based alloys have been developed for high temperature applications, such as tubes of steam power plant, from very simple Fe-2.25Cr-1Mo steels that only provide about 42% efficiency up to advanced Fe-12Cr based steels containing refractory elements of W, Nb and V that provide carbide particles strengthening and give efficiency of the power plant at about 50% [12]. Higher efficiency might be obtained from nickel based alloys. The Ni-Cr-Al systems are the basic for development of nickel-based superalloys. Other alloying elements such as Ti and Mo may be involved for precipitation of intermetallic compounds, especially γ'-Ni_3(Al,Ti) and carbide precipitates of MC, $M_{23}C_6$, M_7C_3 or M_6C [4]. However, Fe-Ni based alloys with α-ferrite or γ-austenite matrix still attract high attention for high temperature applications since this group of alloys are less expensive compared with Ni-based alloys. Schematic ternary phase diagram of Ni-Fe-Cr system, as shown in Fig. 1, can be used as the basic for development of both iron and nickel based alloys. Various alloy systems may be developed from alloys of rich in Ni up to those rich in Fe, all of which may contain minimum Cr of about 12% for Cr_2O_3 protective scale formation can occur all over the surface of the alloys.
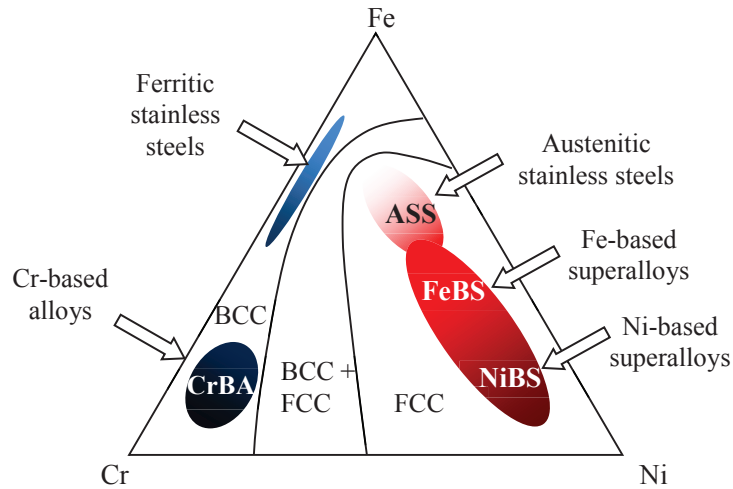
FIGURE 1. Maps of ternary based alloys of Fe-Ni-Cr [13]

Development of B2-(Fe,Ni)Al in α and γ Matrix

The replacement of some Cr with Al as alloying elements are of great interest especially for development of Fe-Ni-Al based alloys [14] as these materials are relatively cheaper, lighter and stronger as a result of the dispersion of intermetallic compound precipitates of B2-(Fe,Ni)Al [15,16]. Investigation on the effect of aluminum addition on the microstructural evolution of Fe-Ni-Al alloys at high temperatures has been recently conducted [17]. Previously Fahmi [18] has studied the Fe-Ni-Al-Cr *i.e.,* Fe-13.7Ni-35Al-2Cr, Fe-13Ni-35Al-5Cr and Fe-12Ni-35Al-10Cr (all composition are in weight percent unless stated otherwise). The materials were made from low carbon FeNi shots containing 76.7 wt.%Fe, 22.7 wt.%Ni, 0.3 wt.%Co, 0.1 wt%Cr, 0.1 wt%Si, 0.01 wt.%C, 0.01 wt.%P and 0.017 wt.%S produced by PT. Antam Tbk. and pure aluminium ingot obtained from PT. Inalum Indonesia. Melting in a single electrode DC arc furnace purged with high purity argon was carried out for preparing the alloys. The as-cast alloys were homogenized at 1100ºC in an electrical tube furnace in an argon atmosphere. Figure 2 shows the buttons of as homogenized alloy samples. Fahmi [18] obtained two important intermetallic compounds of (Fe,Ni)₃Al as the matrix and (Fe,Ni)₂(Al,Cr) as precipitate (Fig. 3). Since these materials are brittle, Fitriani [17] selected chemical composition of Fe-21Ni-14Al, Fe-21Ni-17Al and Fe-21Ni-20Al in order to obtained high concentration of B2-(Fe,Ni)Al in the matrix of α-Fe and γ-Fe. After solution treated at 1100ºC, all samples were aged at 600, 700 and 800ºC for 6, 12, 24 and 36 hours. All alloys contain B2-(Fe,Ni)Al phase, one of which is shown in Fig. 4. This study revealed that addition of Al into FeNi promote transition of the intermetallic precipitates, varied from NiAl, FeAl, and (Ni,Fe)Al. The matrix of γ-Fe was found in the alloy of highest Al content, *i.e.,* Fe-21Ni-20Al. However, as seen in Fig. 4, large size B2-(Fe,Ni)Al occurred.

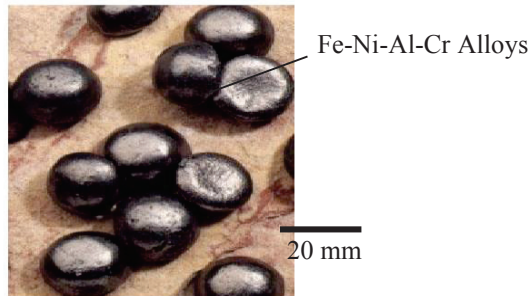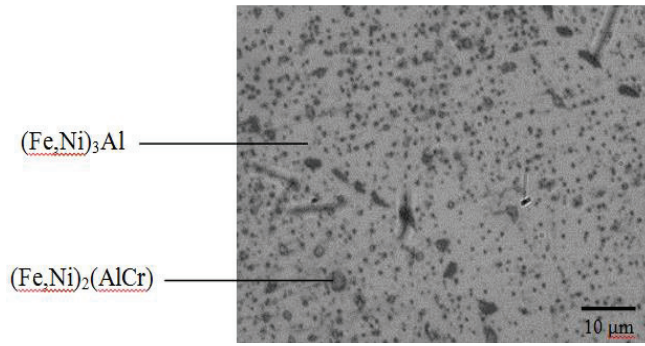**FIGURE 2.** Some alloy buttons after melting in a single electrode DC arc furnace [18]

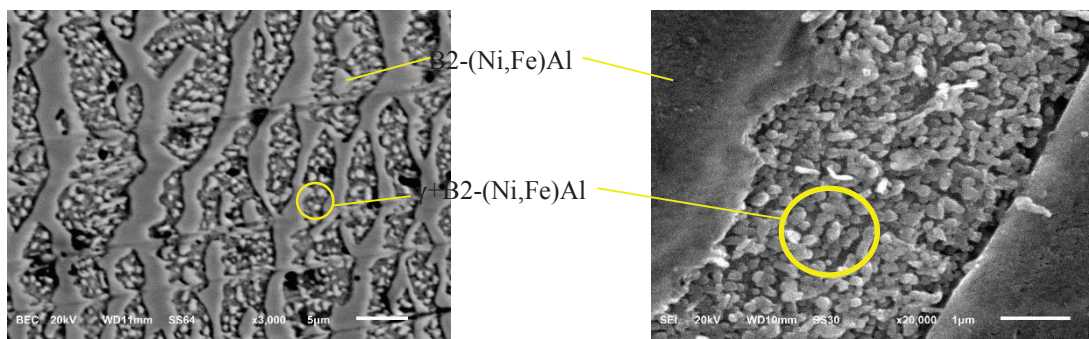**FIGURE 3.** Microstructure of Fe-13Ni-35Al-5Cr after ageing at 700ºC for 4 hours

FIGURE 4. Electron micrographs of Fe-21Ni20Al aged at 700ºC for 24 hours [17]

To avoid large size of B2-(Fe,Ni)Al phase and to obtain α-Fe matrix, Fantowi [19], Adli [20] and Yanas [21] investigated the development of Fe-Ni-Al-Cr based alloys of Fe-16Ni-9Al with different Cr content of 2.5%, 5% and 7.5%. To develop very fine precipitates, the alloys were solution treated at 1100ºC and aged for various times at 650, 750 and 850ºC. Due to the limited space available, only few results were presented in this paper. Figure 5 shows nano size rounded cuboidal B2-(Fe,Ni)Al precipitates distributed homogenously in the matrix of α-Fe. The alloy had chemical composition of Fe-16Ni-9Al-5Cr. The particle size, however, varied from very small size up to about 500 nm, with the average of roughly 180 nm. The precipitates have crystallographic orientation of <100> since the ferrite matrix has body centered cubic. The study also showed that the morphology and the volume fraction of the B2-(Fe,Ni)Al phase varies with the chromium content in the alloys. Since Cr is a ferrite stabilizer, increasing Cr content in the alloys reduces the B2-(Fe,Ni)Al volume fractions. The volume fraction of the B2-(Fe,Ni)Al reduces in alloy containing higher Cr, such those find in Fe-16Ni-9Al-7.5Cr. Moreover, the secondary B2-(Fe,Ni)Al precipitates coarsened during ageing resulted in the consumption of surrounding smaller B2-(Fe,Ni)Al precipitates as shown in Fig. 6. Similar with that Stallybrass has previously informed, this study also found that rounded - cuboid occur when the volume fraction less than about 20% and tend to be elongated when the volume fraction increases, as schematically shown in Fig. 7.
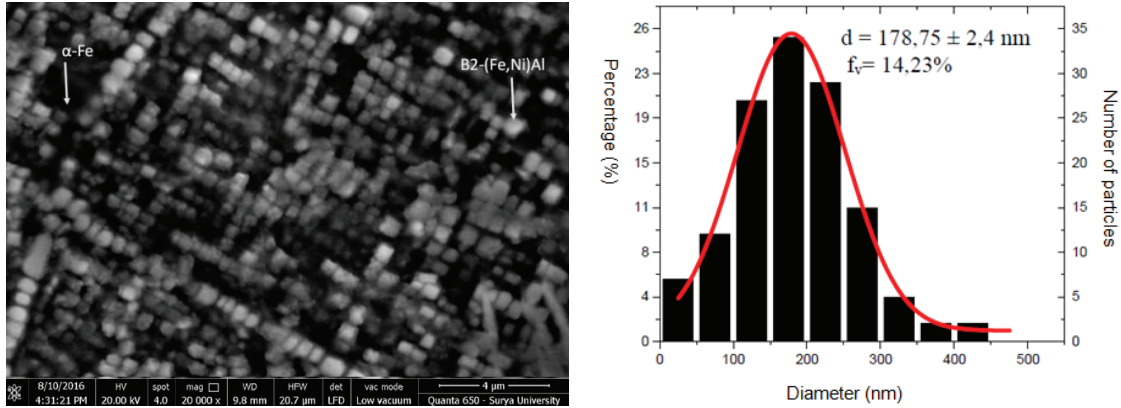
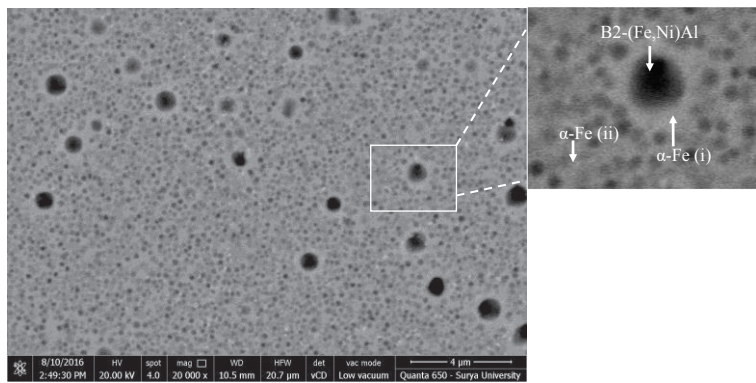**FIGURE 5.** Rounded cuboidal of B2-(Fe,Ni)Al precipitates [19]

FIGURE 6. Primary and secondary B2-(Fe,Ni)Al precipitates in the sample after *ageing* at 650 °C for 48 hours [21]

Development of ODS Ferritic Steels

Coarsening of B2-(Fe,Ni)Al precipitates in ferrite matrix as well as other precipitates, such as carbides and γ'-Ni$_3$(Al,Ti) have been found [21,3]. This can occur at high temperatures due to the tendency of alloys to reduce their free energy. Consequently, the strength of the alloys decreases with time of operation since the distance between particles widen with time. However, for oxide particles such as Y$_2$O$_3$, ThO$_2$ or ZrO$_2$ dispersed homogeneously in the alloy matrixs, due to their extremely low solubility in the matrix, they would not coarsen at high temperatures. Therefore, these systems have been considered very effective for high temperature strengthening.

FIGURE 7. Effect of B2-(Fe,Ni)Al precipitates volume fractions on their morphology [15,20]

The oxide dispersion strengthening (ODS) with nano size oxide particles dispersed homogenously in the matrix of ferrite have been studied recently studied [22,23,24,25,26]. Three different ODS alloys of Fe-16Cr-0.4Y_2O_3, Fe-16Cr-4Al-0.4Y_2O_3 and Fe-16Cr-4Al-1Ni-0.4Y_2O_3 were selected in this study. The ODS alloys were produced using mechanical alloying method. The powder mixtures of base metals, alloying elements as well as oxide powders were milled for different times of 30, 60, 90 and 120 minutes in a planetary ball mill. The milled powder of each sample was then compacted using cold pressing and sintered at different temperatures of 800 and 1000°C. It was found that powder milled for longer times made difficult for cold compaction. However, annealing of the milled powder increased the ability for the powder to be compacted. The x-ray diffraction test result (Fig. 8) revealed that milled powders of all samples have been homogenously alloyed producing matrixes of α-Fe. Even-though relatively difficult to observe using SEM, it is believed that fine Y_2O_3 particles embedded inside of alloy milled powder. Cold compaction and sintering of the milled powders at high temperatures joint the powders and reduce the pores, as shown in Fig 9. The powder milled for longest time (120 minutes) gave high pores due to the limited ductility available for the alloy powders to be deformed during cold compaction (Fig. 9. (b)).
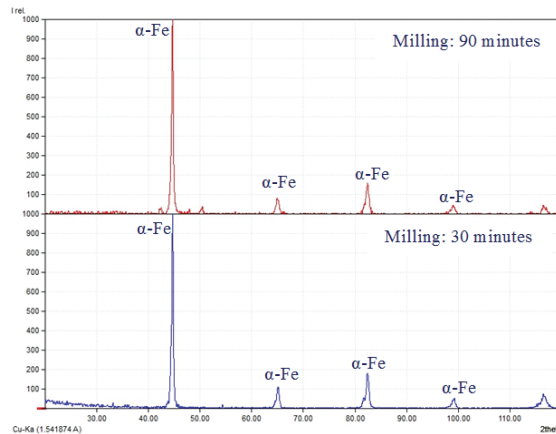

FIGURE 8. XRD analysis results indicate formation of ferrite α-Fe in mechanically alloyed powders [24]
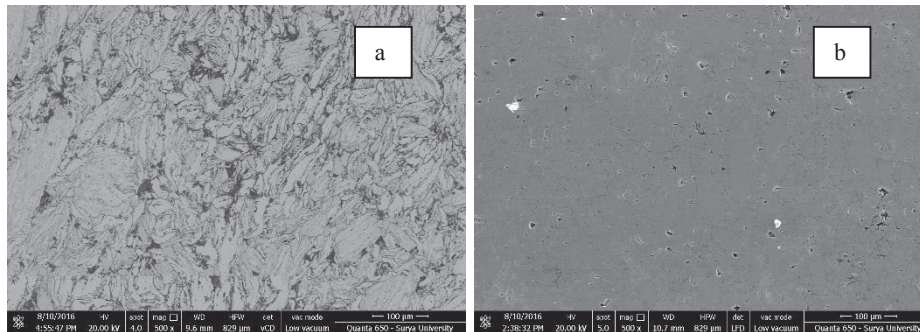

FIGURE 9. Microstructures of ODS, (a) after milling for 120 minutes and sintering at 800°C for 6 hours, (b) after milling for 30 minutes and sintering at 1000°C for 6 hours [25]

Superalloys

Superalloys are defined as materials based on the VIIIA group of the periodic table and developed for high temperature applications in which a good combination of strength and oxidation resistance at high temperatures (T ≥800°C) is required. There are basically three types of superalloys i.e., iron-based, nickel-based and cobalt-based superalloys. Among these three, nickel-based superalloys give better high-temperature performance and are therefore widely used as turbine blade materials in aero engines. Various alloying elements have been involved in these three superalloys, each of which with its role, either for strengthening, corrosion resistance and phase stability. Nickel-based superalloys are basically strengthened by coherent precipitates of the ordered intermetallic γ'-Ni_3(Al,Ti). This phase

has unique mechanical properties in which the strength increases with temperature up to about 900°C. Further development of nickel-based superalloys involved the addition of some other elements such as carbon to form carbide precipitates, odd size elements such as boron and zirconium to strengthen the grain boundaries, and other solid solution elements such as cobalt and refractory elements (e.g., molybdenum and tungsten) which increase the melting point of the alloys as well as solid solution strengtheners.

Nickel based superalloys with basic chemical composition of Ni-12Al-9Cr-4Ti-Mo and different Mo has been developed [27]. Figure 10 shows one of the microstructure found in Ni-11.1Al-9Cr-3.6Ti-2.2Mo. Primary and secondary γ'-Ni$_3$(Al,Ti) precipitates were found in the alloys. Secondary γ' precipitates only provide minor benefit for strengthening in nickel based superalloys because of their large sizes, but usually could not be avoided. This study revealed that increasing the Mo content reduced the secondary γ' precipitates in nickel based superalloys.
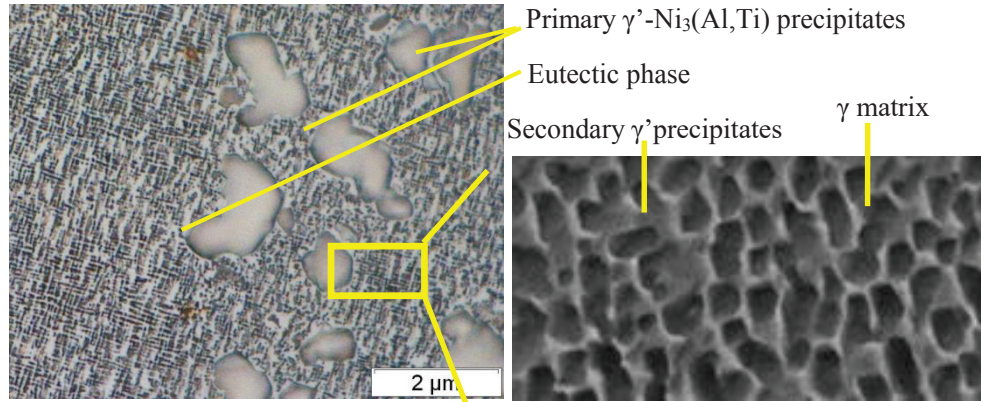
FIGURE 10. Microstructure of Ni-11,1Al-9Cr-3,6Ti-2,2Mo and corresponding EDS patterns for matrix and γ'-Ni$_3$(Al,Ti) precipitate [27]

Addition of minor elements such as Y, Zr and Hf has been intensively studied and these elements are believed increase the adherence of the protective scales. Effect the addition of Ge in Ni-21Cr-2,7Ti-0,9Al-0.05C and Ge and Zr in Ni-5.60Al-9.60Cr-2.4Ti-0.05C on the oxidation behavior at 1100°C was recently carried out [28,29]. The Ge and Zr addition was varied up to 2%. The oxidation tests were performed in isothermal as well as cyclic oxidation at 1100°C. It was revealed that while Zr improve the spalling resistance, Ge only significantly provide improvement of oxide spalling when its concentration is less than 2%. Similarly, the kinetic study of isothermal oxidation indicated that contribution of Ge on the reduction of oxidation rate only significant for addition of less than 1%. Nevertheless, general parabolic behavior of oxidation was found for all alloys studied. The XRD patterns shown in Fig.12 confirmed that several oxides of Al$_2$O$_3$, Cr$_2$O$_3$, TiO$_2$ and spinel of NiCr$_2$O$_4$ were formed. The X-ray mapping of the scale, as depicted in Fig 11, shows internal oxidation, mostly dominated by oxides of TiO$_2$ and Al$_2$O$_3$, while outer layer of the scale occupied by Cr$_2$O$_3$ and spinel of NiCr$_2$O$_4$. Relatively thin oxide layer of TiO$_2$ on the outer part of the scale was resulted from early oxidation. However, the protective oxide of Cr$_2$O$_3$ progressively replaced TiO$_2$.
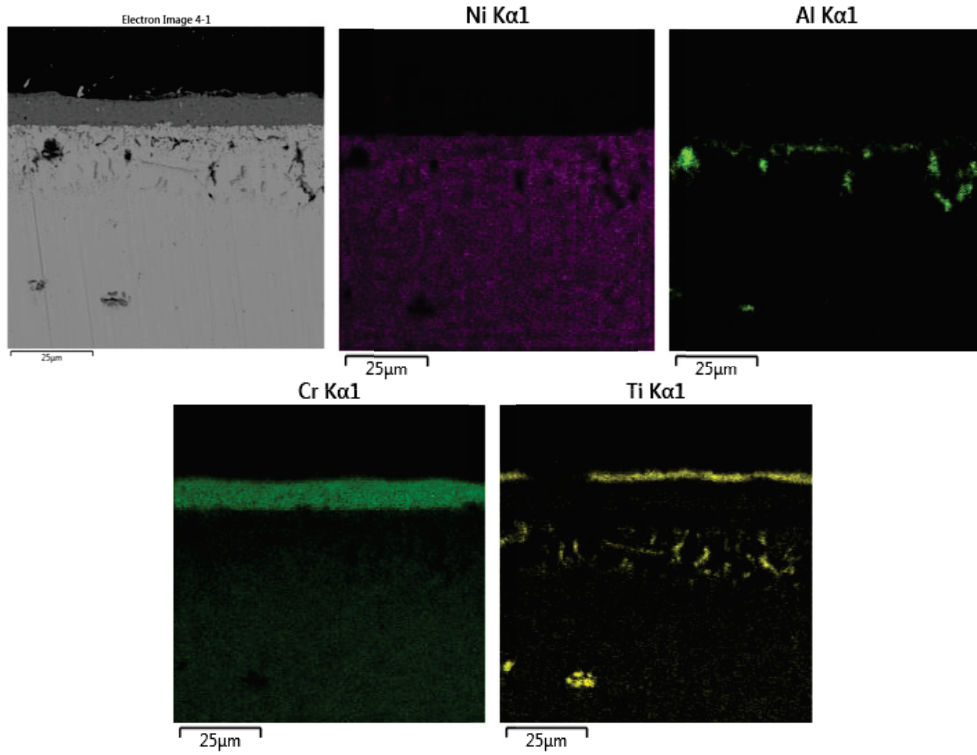
FIGURE 11. Microstructures of scales formed on Ni-21Cr-2,7Ti-0,9Al-0.05C-2Ge alloy after isothermal oxidation at 1100°C for 48 hours and corresponding X-ray mappings

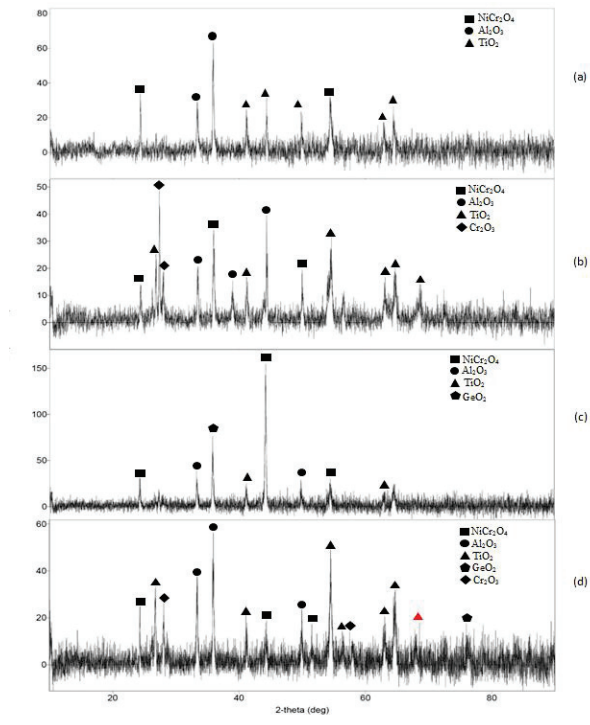
FIGURE 12. XRD patterns of scales on alloys after isothermal oxidation at 1100°C. (a) No Ge after oxidation for 2 hours, (b) No Ge after oxidation for 48 hours, (c) 2% Ge after oxidation for 2 hours, and (d) 2% Ge after oxidation for 48 hours

TWO PHASE α_2-Ti$_3$Al/γ-TiAl INTERMETALLIC COMPOUNDS

Oxidation of α_2-Ti$_3$Al/γ-TiAl Alloys

Aluminide based intermetallic compounds, such as FeAl, NiAl and TiAl alloys, have been considered as candidates for high temperature alloys since they have high aluminium contents to provide protective alumina scale. However, these materials are brittle, and therefore, efforts to increase ductility have been intensively carried out [30]. TiAl based alloys attract higher attentions due to their lower density so they give higher strength to weight ratio and suitable for replacement of nickel-based superalloys used in aero turbine engines. Utilization of two phase α_2-Ti$_3$Al/γ-TiAl as the base for TiAl alloys provides TiAl base alloys with relatively less brittle. Nevertheless, these materials are relatively poor in oxidation resistance due to lower aluminium content in the alloys. Coatings based on TiAl$_3$ have been widely applied to improve their oxidation resistant [31,32].

Effect of Cr addition as third alloying element in two-phase intermetallic alloys of α_2-Ti$_3$Al/γ-TiAl on oxidation resistance have been studied [33]. The addition of Cr was expected to improve the formation of stable Al$_2$O$_3$ and increase the oxidation resistance of the titanium aluminide alloys. The chemical composition of the alloys was varied with the base alloys of Ti-48Al and chromium content from 1%, 1.5% up to 2%. Isothermal oxidation test was performed at 800, 900 and 1000°C for various times up to 45 hours. This study showed that addition of 1% up to 2% Cr reduced the growth rate of TiO$_2$ and increase Al$_2$O$_3$ scale at alloy surface. As shown in Fig 13 (b) the TiO$_2$ oxide was formed at surface (Fig. 13 (c)) when no Cr was involved. Addition of 2% Cr provide outer layer of Al$_2$O$_3$, while Al$_2$O$_3$ and Cr$_2$O$_3$ oxide was found underneath of TiO$_2$ layers when relatively small amount of Cr of about 1% is added (Fig. 13 (d)).
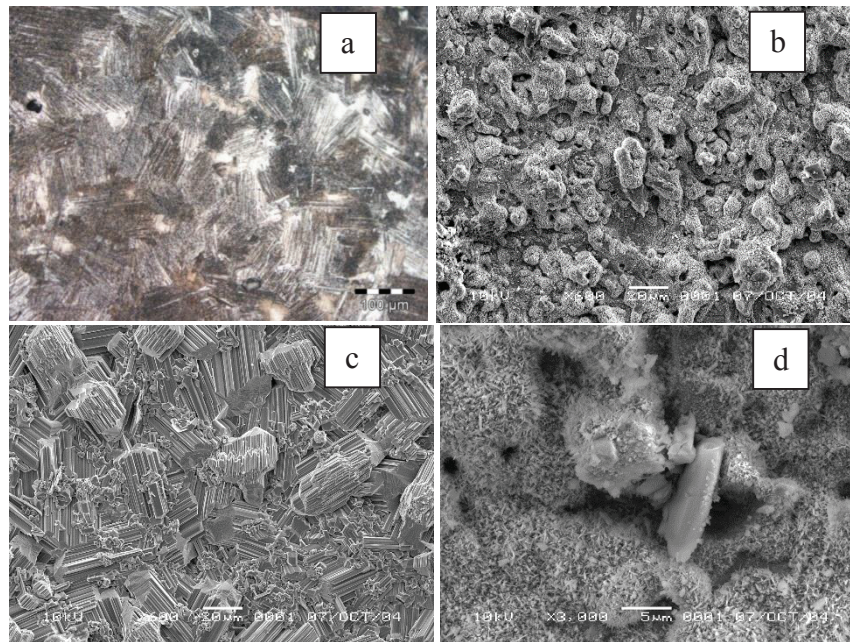

FIGURE 13. (a) Microstructure of α_2-Ti$_3$Al/γ-TiAl, (b) oxide of Al$_2$O$_3$, (c) oxide of TiO$_2$ and mixed oxides of Al$_2$O$_3$ and TiO$_2$ [33]

Effect of Ag and Cr addition on the oxidation behavior of two phase α_2-Ti$_3$Al + γ-TiAl in TiAl based alloys have been investigated [34]. These two alloying elements were expected to have reservoir-effect that supports the formation of continuous stable Al$_2$O$_3$ scale as reported previously in single phase TiAl intermetallic compounds [35,36,37]. In this alloy systems, chromium can act as Laves phase-Ti(Cr,Al)$_2$ stabilizer while silver stabilizes Z phase-Ti$_5$Al$_3$O$_2$. Three alloys have been prepared 48Ti-50Al-1.5Ag-0.5Cr, 48Ti-49Al-1.5Ag-1.5Cr and 48Ti-47.5Al-1.5Ag-3Cr. Isothermal oxidation tests were carried out at 850°C for various times of 2, 10, 15 and 20 hours. Fig. 14 shows the microstructure of the sample containing 3% Ag after oxidation test for 20 hours. The XRD pattern of the surface indicates the mixture of TiO$_2$ and Al$_2$O$_3$. It was expected that both Cr and Ag decrease diffusivity of Ti in the scales, and reduce the formation of un-protective TiO$_2$. Moreover, addition of Ag and Cr induce the formation of intermixed of Laves phase

Ti(Al,Cr)$_2$, Z phase (Ti$_5$Al$_3$O$_2$) and Ag-rich precipitates as the inner layer. In the middle, intermixed of majorly TiN and minor of TiO$_2$ and Al$_2$O$_3$ were formed. This TiO$_2$ occurred when some TiN oxidized [36]. Longer times as well as higher oxidation temperatures might change the scale compositions.

High Temperature Coatings on TiAl Based Alloys

Pack aluminizing on TiAl alloys have been intensively studied especially to provide high concentration of Al for Al$_2$O$_3$ scale formation on the alloy surface. Coatings on α_2-Ti$_3$Al + γ-TiAl alloys essentially important due to relatively low Al content in the alloys. Comprehensive pack aluminizing study have been conducted on a α_2-Ti$_3$Al + γ-TiAl alloy containing TI-47Al-2Nb-2Cr-0.5Y-0.5Zr [38]. The pack filler contained aluminum powder as the master alloy, NH$_4$Cl as the activator and Al$_2$O$_3$ as the inert filler. Composition of Al varied by 25%, 30 % and 35 %, all in weight percent, while the activator NH$_4$Cl was varied at 4%, 6 % and 8 % and balance for Al$_2$O$_3$. Pack aluminizing processes were carried out at 900ºC for 10 hours. Continuous coatings of TiAl$_3$ on the α_2-Ti$_3$Al + γ-TiAl alloys with various thicknesses can be obtained, one of which shown in Fig. 15. Thermodynamically, a layer of TiAl$_2$ should be formed. However, no such phase layer was identified, probably due to extremely thin layer of this phase.
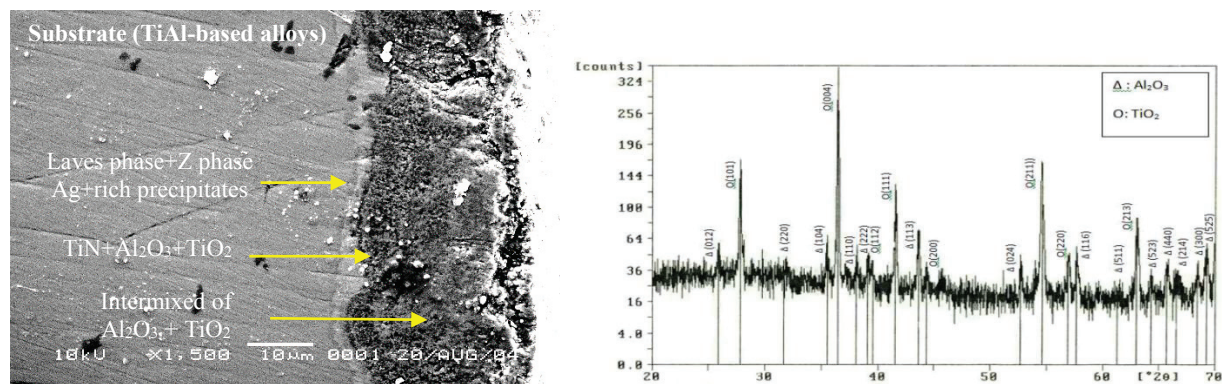
FIGURE 14. Microstructure of alloy containing 48at%Ti-47.5at.%Al-1.5at.%Ag-3at.%Cr after oxidation test at 850ºC for 20 hours and corresponding XRD pattern of the surface scale

The EDS analysis confirmed that Zr, Cr and Nb contained in the layer of TiAl$_3$ for all coatings produced. However, for certain coatings, no Yttrium was found in this coating layer. This fact indicates that in TiAl$_3$ diffusion of Zr, Cr and Nb is relatively high while Y diffuses slowly. Moreover, the solubility of Y is believed very low due to high different in atomic size with that of Ti. Nevertheless, it was found that some coatings contain precipitates. Large amount of precipitates was found in coating with pack composition of 35Al-2NH$_4$Cl as shown in Fig. 15 (b). Different chemical compositions were identified in some different precipitates, but mostly they are rich in Y, i.e., Al$_{65}$, Ti$_3$, Cr$_2$, Y$_{25}$, Zr$_2$, Nb$_3$ and Al$_{19}$, Ti$_2$, Y$_{64}$, Zr$_6$, Nb$_9$. The occurrence of Y in the coating is predicted increases the ductility of the TiAl$_3$ coating layer [32].
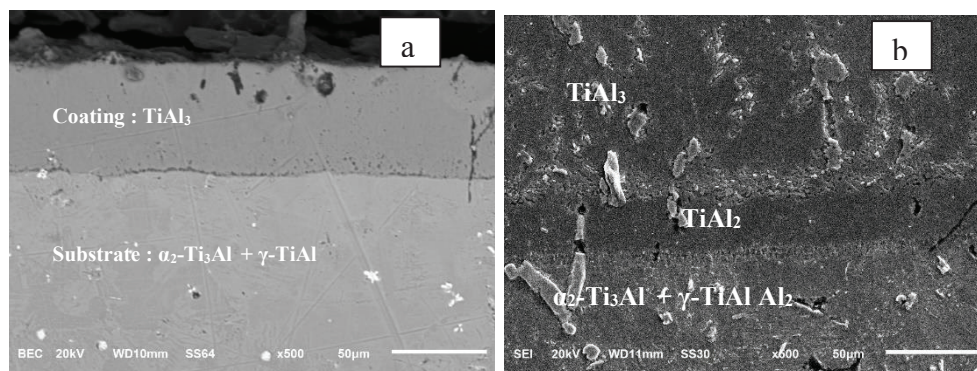
FIGURE 15. (a) Layer of TiAl$_3$ on substarte of α_2-Ti$_3$Al + γ-TiAl, and (b) large precipitates found in a coating

High Temperature Oxidation of Coated α₂-Ti₃Al/γ-TiAl Alloys

Cyclic oxidation of α₂-Ti₃Al/γ-TiAl has been studied[39]. The intermetallic α₂-Ti₃Al/γ-TiAl alloy were prepared with the chemical composition of 47 at.Al, 2 at.% Nb, 2 at.% Cr, 0.5 at.% Zr, 0.5 at.% Y and balance of Ti. Pack cementation process was done with pack composition of 78 wt.%Al₂O₃, 20 wt.%Al and 2 wt.% NH₄Cl at 900ºC for 10 hours. The oxidation tests were carried out at 1000, 1050, and 1100ºC up to 20 cycles. Each cycle consists of 1 hr. heating at atmospheric environment and fast cooling to room temperature and held for 15 minutes before continuous heating at the same time and temperature. It was found that spallation occurred during oxidation in all un-coated samples. The spalled oxides consist mostly of TiO₂ and small amount of Al₂O₃. Figure 16 (a) shows the microstructure of the coated sample after oxidation at 1100ºC for 20 cycles. High adherence of scales, however, was found in all coated samples as shown in Fig. 16 (b). The scales predominantly consist of Al₂O₃ and slight amount of TiO₂ and Cr₂O₃. At 1100ºC, some Cr₂O₃ might have oxidized into volatile CrO₃. It was found that Ti₂AlN occurred in the samples after cyclic oxidation at 1100ºC for 20 cycles. The occurrence of Ti₂AlN on the scale can be related with earlier study [40] on the thermodynamics of Ti-Al-N at 1273 K. These researchers reported that Ti₂AlN is in the equilibrium with TiN and α₂-Ti₃Al or γ-TiAl. Therefore, it seems that the Ti₂AlN should be formed on substrate-oxide interface. The occurrence of Ti₂AlN on the surface of the oxide scale is predicted due to the reaction between TiN and Al₂O₃, or alternatively as the results of reaction between TiN and TiAl₃ as the matrix of the coating. Even-though the mechanism of nitride formation on the surface has not been clearly revealed, it is confirmed that this nitride alters the formation of Al₂O₃ in the outer scale. This study also found that addition of Y and Zr in the alloy increase the adherence of scales.
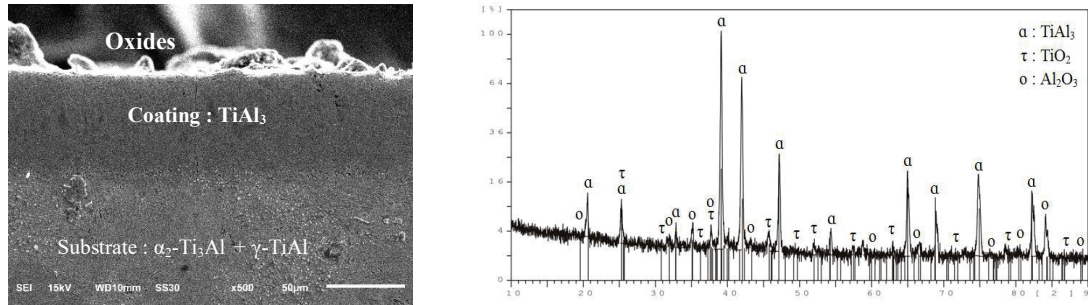
FIGURE 16. XRD pattern of aluminide coatings of pack aluminisde coated two phase α₂-Ti₃Al + γ-TiAl (a) in as coated sample, (b) after oxidation at 1000ºC for 24 hours
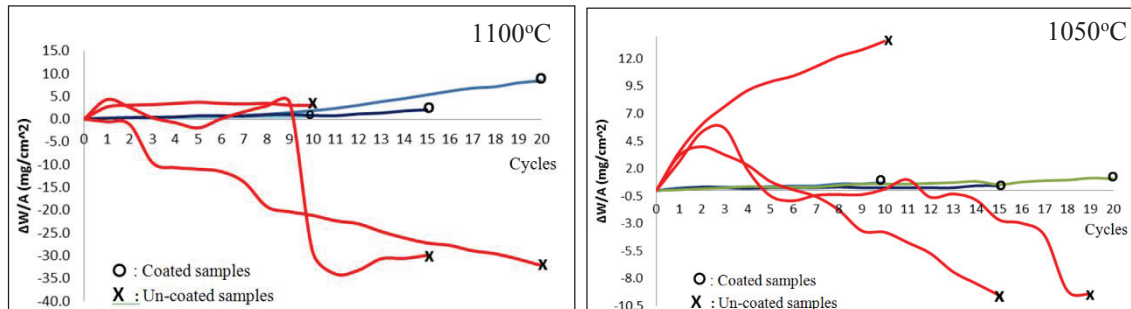
FIGURE 17. Weight changes of coated and un-coated α₂-Ti₃Al or γ-TiAl samples after cyclic oxidation test at 1100ºC and 1050ºC

Hot Corrosion of Coated Alloys

A series of experiment on pack aluminizing and hot corrosion were done on substrate of Ti-47Al-2Nb-2Cr-0.5Zr-0.5Y intermetallic alloys [41]. The composition of pack alumizining is 2% NH₄Cl, 20% Al and 78% Al₂O₃. These aluminizing processes resulted TiAl₃ phase rich in Al as the main coating. The hot corrosion tests were done to coated alloys at various temperatures and times, i.e., 700ºC, 800ºC, 900ºC and 2, 5, 10, 22 hours. The tests were done by immersing or submerging the coated sample coupons in a molten salt containing 90% Na₂SO₄ and 10% NaCl.

Characterization of corrosion products using XRD and SEM/EDS confirmed that oxide mixture of $TiAl_3$, Al_2O_3, TiO_2, TiO, Nb_2O_5 were found on the surface of the samples.
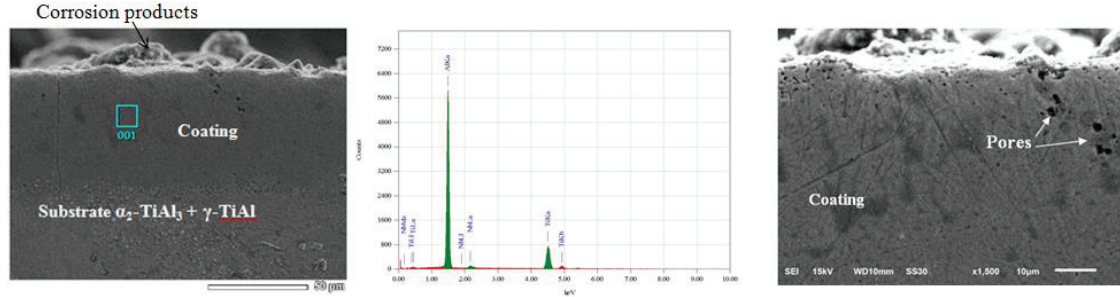
FIGURE 18. Microstructure of coated samples after hot-corrosion test at 800°C for 22 hours

Generally, it was found that the coated specimen had better resistance for spallation and corrosion resistance. Nevertheless, it was found that some pitting occurred on the outer parts of some coatings, as shown in Fig. 18 (b). Pitting has been recognized as the degradation of coating due to the consumption of metals atoms by chloride gas. Scale containing TiO_2 and Al_2O_3 will simultaneously form at early oxidation of coated samples. These oxides, however, react with molten salts [42,43] according the following reactions:

$$Ti + O_2 \rightarrow TiO_2 \tag{2}$$

$$2Al + 3/2\ O_2 \rightarrow Al_2O_3 \tag{3}$$

$$2NaCl + Al_2O_3 \rightarrow 2NaAlO_2 + Cl_2 \tag{4}$$

$$NaCl + TiO_2 + O_2 \rightarrow NaTiO_4 + \frac{1}{2}\ Cl_2 \tag{5}$$
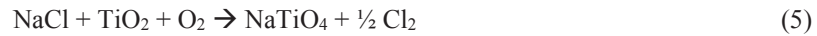
The chloride gas from Eq. (4) and (5) diffuses inwardly through micro cracks and pores of the scale reacts with Ti and Al forming volatile metallic halides according to Eq. (6) and (7).

$$Ti + Cl_2 \rightarrow TiCl_2 \tag{6}$$

$$Al + 3/2\ Cl_2 \rightarrow AlCl_3 \tag{7}$$

The halide vapors diffuse outwardly to the scale surface and finally oxidized forming non protective porous scales.

$$TiCl_2 + O_2 \rightarrow TiO_2 + Cl_2 \tag{8}$$

$$2AlCl_3 + 3/2\ O_2 \rightarrow Al_2O_3 + 3Cl_2 \tag{9}$$

The chloride gas can further diffuse inwardly and similar mechanism of Ti and Al halide gas formations may occur resulted in the formation of pitting and pores and increase the corrosion rate.

Interdiffusion Between Coatings and Substrates

Application of pack aluminide coated alloys at high temperatures can lead to interdifusion of elements in the coating and substrate, and this make the coating thickness decreasing with time and reduce the life of the coatings. Interdiffusion between the aluminide coatings and substrate of nickel based superalloys have been intensively studied [44,45,46]. However, few studies focusing on the interdiffusion of pack aluminide coated two phases α_2-Ti_3Al+γ-TiAl intermetallic alloys. Recently, studies on interdiffusions on coated TiAl based alloys of Ti-47Al-2Cr-2Nb-0.5Zr-0.5Y at 800, 900 and 1000°C have been carried out [47,48]. A new layer of $TiAl_2$ occur as interdiffusion layer between the coating of $TiAl_3$ with the alloys, mainly as the results of outward diffusion of Ti and inward diffusion of Al. Prediction

of parabolic growth rate for the $TiAl_2$ layer formation were followed with increasing rate for higher temperatures. The study also revealed that the addition of micro alloying elements of Nb, Cr, Zr and Y significantly reduce the interdiffusion layer growth and increase the lifetime of main coating layer of $TiAl_3$ at high temperatures. Efforts to reduce further the interdiffusion rate by developing a protective layer underneath the $TiAl_3$ coatings is still being carried out.

CONCLUDING REMARKS

Comprehensive understanding on microstructural changes and high temperature oxidation/corrosion has been the issues in the development of high temperature alloys. These alloys have relatively low content of Al and Cr for corrosion protection at high temperatures. This issue has been addressed by involving diffusion coatings rich mostly in Al. Nevertheless, oxidation and hot corrosion of the coating, especially on TiAl systems, requires very high Al content, which is $TiAl_3$ that relatively brittle. Moreover, for all aluminide coated systems studied, the coating life time depends on the availability of Al and Cr to provide protective scales of Al_2O_3 and Cr_2O_3. Interdiffusion between coatings and alloy substrates, however, reduces the Al and Cr content in the coating. Alloying has been found to play an important role in addressing this problem. Preliminary study on the development of ODS ferritic steels has revealed that milling using planetary ball mill in relatively short time of only 30 minutes can provide homogenous mechanical alloying of α-Fe. Very long times of milling, however, reduce the ability for milled green powder to consolidate during compaction and sintering. Annealing of the milled powder is expected reduce this problem. More extensive studies need to be done in order to find more effective ways to increase life times and operating temperatures of the alloys.

REFERENCES

1. Viswanathan R., Purget R., Rao U., "Materials for ultra-supercritical coal-fired power plant boilers", in *Proceedings of the 7th Liege Conference on Materials for Advanced Power Engineering*, (Forschungszentrum Jülich, 2002), Vol. 21, Part I-III, pp.1109-1129.
2. C.A. Estrada, Scientia Et Technica **13** (36), 297-301 (2007).
3. R.C. Reed, *The Superalloys: Fundamentals and Applications*, (Cambridge University Press, New York, 2006).
4. C.T. Sims, *Superalloys II: High-Temperature Materials for Aerospace and Industrial Power*, edited by C.T. Sims, N.S. Stoloff, and W.C. Hagel, (John Wiley & Sons Inc., 1987).
5. C. Suryanarayana, Progress in Material Science **46** (1-2), 1-184 (2001).
6. G.W. Goward, Surface Coatings Technology **108-109**, 73-79 (1998).
7. J. Stringer, Materials Science Technology **3** (7), 482-493 (1987).
8. R.A. Rapp, Corrosion **42** (10), 568-577 (1986).
9. J.A. Goebel and F.S. Pettit, Metallurgical Transactions **1** (7), 1943-1954 (1970).
10. F.S. Pettit, and G. H. Meier, *Oxidation and Hot Corrosion of Superalloys*, (The Metallurgical Society of AIME, Warrendale, PA, 1984) pp. 651-687.
11. P.C. Patnaik and J.P. Immarigeon, *High Temperature Protective Coatings for Aero Engine Gas Turbine Components*, (National Research Council Canada, 1985) NRC No. 26475.
12. F. Masuyama, "Trends in power engineering in Japan and requirements for improved materials and components", in *Proceedings of the 7th Liege Conference on Materials for Advanced Power Engineering*, (Forschungszentrum Jülich, 2002), Vol. 21, Part I-III, 2002, pp. 1767-1782.
13. T. Jonsson, S. Canovic, F. Liu, H. Asteman, J.E. Svensson, L.G. Johansson, M. Halvarsson, Materials at High Temperatures, **22** (3-4), 231-243 (2005).
14. V. Raghavan, Journal of Phase Equilibria and Diffusion **31** (5), 455-458 (2010).
15. C. Stallybrass and G. Sauthoff, Materials Science and Engineering A **387-389**, 985-990 (2004).
16. C. Stallybrass, A. Schneider, and G. Sauthoff, Intermetallics **13** (12), 1263-1268 (2005).
17. C. A. Fitriani and E. A. Basuki, "Microstructural evolution and oxidation behavior of Fe-Ni-Al alloys at high temperatures", presented in *Proceeding International Seminar of CHEMMPRO 2014*, (Institut Teknologi Bandung, 2014).
18. A. Fahmi, "The effect of Cr addition on the microstrostructure of Fe-Ni-Al alloy at high temperature", Undergraduate thesis, Institut Teknologi Bandung, 2004
19. I. Fantowi, "Strengthening behaviour of nano-coherent B2-(Fe,Ni)Al precipitates in advanced ferritic steels", Undergraduate thesis, Institut Teknologi Bandung, 2016.

20. A.I. Adli, "Phase transformation of B2-(Fe,Ni)Al precipitate in advanced ferritic Fe-14Ni-5Cr-9Al steels under aging condition", Undergraduate thesis, Insitut Teknologi Bandung, 2016.
21. Y.G. Yanas, "Precipitation of nano B2-(Fe,Ni)Al phase in advanced ferritic steels", Undergraduate thesis, Institut Teknologi Bandung, 2016.
22. G. Sundararajan, R. Vijay, and A.V. Reddy, Current Science **105** (8), 1100 (2013).
23. H. L. Ding, R. Gao, and T. Zhang, Fusion Engineering and Design **100**, 371–377 (2015).
24. S. Ardiansyah, "Effect of milling time and sintering temperatures on the microstructures and mechanical properties of oxide dispersion strengthened (ODS) ferritic Fe-16Cr-0.4Y_2O_3 steels", Undergraduate thesis, Institut Teknologi Bandung, 2016.
25. A. M. A. Khan, "Effect of milling time and sintering temperatures on the microstructure evolution of oxide dispersion strengthened Fe-16Cr-4Al-1Ni-0.4Y_2O_3", Undergraduate thesis, Institut Teknologi Bandung, 2016.
26. F. Ramaputra, "Study of oxide dispersion strengthened (ODS) ferritic steels making (Fe-16Cr-4Al-0.4Y_2O_3) by mechanical milling methods", Undergraduate thesis, Institut Teknologi Bandung, 2016.
27. G.A. Tambunan, "Effect of Ti and Mo additions on the microstructure stability of Ni-based superalloys", Undergraduate thesis, Institut Teknologi Bandung, 2010.
28. F. Adam, "Effect of germanium addition on the isothermal oxidation resistance of Ni-21Cr-2.7Ti-0.9Al superalloys at temperature 1100°C", Undergraduate thesis, Insitut Teknologi Bandung, 2016.
29. F. Pangestu, "Effect of Ge and Zr addition on the oxidation resistance of nickel-based superalloy at 900, 1000 and 1100°C", Undergraduate thesis, Institut Teknologi Bandung, 2016.
30. S.P. Brookes, Thermo-Mechanical Fatigue Behaviour of the Near-γ-Titanium Aluminide Alloy TNB-V5 Under Uniaxial and Multiaxial Loading. Ph.D. thesis, Federal Institute for Materials Research and Testing (BAM), 2009.
31. K. Kothari, R. Radhakrishnan, N. Wereley, Progress in Aerospace Sciences **55**, 1-16 (2012).
32. S.C. Kung, Oxidation of Metals **34** (3), 217-228 (1990).
33. Pawawoi, E.A. Basuki, "Pengaruh unsur khrom (Cr) terhadap perilaku pembentukan oksida paduan TiAl-Cr pada 900°C", in *3rd Indonesian Process Metallurgy Conference (IPM III)*, (Insitut Teknologi Bandung, Bandung, 2012).
34. A. Senaputra, "Study on the isothermal oxidation resistance of two phase alloy γ-TiAl/ $α_2$-Ti_3Al at variation of Ag and Cr addition at temperature of 850 °C", Undergraduate thesis, Institut Teknologi Bandung, 2006.
35. L. Niewolak, K. Lawson, P. Roβbach, E. Wessel, V. Shemet, J.R. Nicholls, L. Singheiser, and W.J. Quadakkers, Materials at High Temperature **20** (4), 631-637 (2003).
36. M.P. Brady, B. Gleeson, I. G. Wright, Journal of Metals **52** (1), 16-21 (2000).
37. L. Singheiser, L. Niewolak, U. Flesch, V. Shemet, and W.J. Quadakkers, Metallurgical and Materials Transactions A **34** (10), 2247-2251 (2003).
38. F. Rahman, "Microstructural evolution of packed aluminized coated $α_2$-Ti_3Al + γ-TiAl alloy with variation of pack filler", Undergraduate thesis, Institut Teknologi Bandung, 2014.
39. E. A. Basuki, D. S. Hajar, F. Rahman, and D. H. Prajitno, Procedia Chemistry **16**, 47-52 (2015).
40. J. C. Schuster and J. Bauer, J. Solid State Chem. **53** (2), 260-265 (1984).
41. Fauzi, A., Prajitno, D.H., and Basuki, E. A., "Investigation on hot corrosion behavior of aluminide coated TiAl alloys", in *Proceeding International Seminar of CHEMMPRO 2014*, (Institut Teknologi Bandung, 2014)
42. Z. Tang, F. Wang, and W. Wu, Oxidation of Metals **51** (3), 235-250 (1999).
43. K. Zhang, Z. Li, and W. Gao, Material Letters **57** (4), 834-843 (2002).
44. E.A. Basuki, A. Crosky, and B. Gleeson, Journal of Materials Science and Engineering A **224**, 27-32 (1997).
45. K.V. Dahl, J. Hald, and A. Horsewell, Defect and Diffusion Forum **258**, 73-78 (2006).
46. Y.Z. Liu, X.B. Hu, S.J. Zheng, Y.L. Zhu, H. Wei, and X.L. Ma, Materials and Design **80**, 63-69 (2015).
47. M.I. Juliansyah, "Interdiffusion between aluminide coating and intermetallic alloys of Ti-47Al-2Cr-2Nb-0.5Y at high temperatures", Undergraduate thesis, Institut Teknologi Bandung, 2014 (Accepted to be published in Journal of Engineering Technological Sciences).
48. F. Muhammad, E.A. Basuki, and M.I. Juliansyah, Indonesian Journal of Physics **26** (1), 13-16 (2015).